SMOS ESL 2019-2024
ESL for Geophysical (L3 & 4) data over land ice and sea ice

CryoSat-2/SMOS Algorithm Theoretical Basis Document (ATBD)

Version 2.5

Prepared by	Stefan Hendricks, AWI Robert Ricker, AWI	13/11/2023
Checked by	Lars Kaleschke, AWI	
Released by	Lars Kaleschke, AWI	

Document Information

Contract Information	
Contract Number	4000130567/20/I-BG “SMOS ESL for SMOS Level 1 and Level 2 over Land, Ocean and Ice”
Contract Issuer	ESA/ESRIN

Internal Distribution		
Name	Organization	Copies
Lars Kaleschke Xiangshan Tian-Kunze	Alfred Wegener Institute	1 1

External Distribution		
Name	Organization	Copies
Klaus Scipal Raffaele Crapolicchio	ESA Serco Italia for ESA	1 1
Internal Confidentiality Level		
Unclassified X	Restricted □	Confidential □

Document Version & Changelog

Version	Sections	Description	Data
2.0	All	First delivery of the Algorithm Theoretical Basis Document for SMOS ESL contract	01/10/2020
2.1	All	Updated for service Review #4	21/10/2021
2.2	All	Updated for service Review #5	04/04/2022
2.3	All	Revised version of 2.2	08/08/2022
2.4	All	Updated for CS2SMOS version v2.05	08/12/2022
2.5	All	Updated for CS2SMOS version v2.06	13/11/2023

Applicable Documents

Abbreviation	Name	Description
ATBD_v1	AWI_ESA_CS2SMOS_ATBD_v1.0	Algorithm Theoretical Basis Document
RM_TN	AWI_ESA_CS2SMOS_RM-TN_v1.6	ReadMe-first Technical Note
PDD	AWI_ESA_CS2SMOS_PDD_v1.6	Product Description Document

1 Purpose of this Document

The purpose of this document is to describe scientific algorithms used to generate the SMOS/CryoSat-2 merged product (CS2SMOS). This document is based on the original Algorithm Theoretical Baseline Document [ATBD_v1] of the SMOS & CryoSat-2 Sea Ice Data Product Processing and Dissemination Service project.

The current version of the SMOS/CryoSat-2 merged product is v2.06 and notable changes to earlier versions [ATBD_v1] developed within the SMOS ESL framework are:

1. Daily update rate of CS2SMOS merged products instead of weekly
2. Utilization of CryoSat-2 trajectory data instead of weekly grids
3. Updates of auxiliary input data sets

2 Motivation and Scope of the CS2-SMOS Data Merging

The Soil Moisture and Ocean Salinity (SMOS) mission provides L-band observations, and the ice thickness-dependency of brightness temperature enables to estimate the sea-ice thickness for thin ice regimes, in particular during the freeze-up (Kaleschke et al., 2012). On the other hand, CryoSat-2 (CS2) uses radar altimetry to measure the height of the ice surface above the water level, which can be converted into sea-ice thickness assuming hydrostatic equilibrium. In contrast to SMOS, The CS2 mission was primarily designed to measure the thickness of the perennial and thick first-year ice cover and lacks the sensitivity for thin ice regimes (Wingham et al., 2006).

The complementary nature of the relative uncertainties of CS2 and SMOS ice thickness retrievals has been shown by Kaleschke et al. (2015). Figure 1 illustrates uncertainty maps and the relative uncertainties of CS2 and SMOS monthly means from March 2016. While the SMOS relative uncertainties are lowest for very thin ice, CS2 relative thickness uncertainties are smaller over thick ice and rise asymptotic towards thickness values < 1 m, which is due to the different methodical approach. We acknowledge that systematic errors as due to the usage of a snow climatology as well as snow-volume scattering may alter the uncertainty estimate (Ricker et al., 2014, 2015).

Also, the spatial coverage is of complementary nature due to the different orbital inclinations. Figure 2 shows weekly means of CS2 and SMOS during the freezing season 2015/16. While valid SMOS ice thickness estimates can be found mostly in the marginal ice zones, the CS2 ice thickness retrieval covers major parts of the Arctic multiyear ice (MYI). Figure 3 illustrates the number of valid grid cells of the weekly means as shown in Figure 2. The number of grid cells, which share SMOS and CS2 estimates, is significantly lower than of grid cells that contain thickness estimates from one sensor exclusively.

Therefore, merging of CS2 and SMOS sea-ice thickness retrievals has the capability to complete Arctic sea-ice thickness distributions.

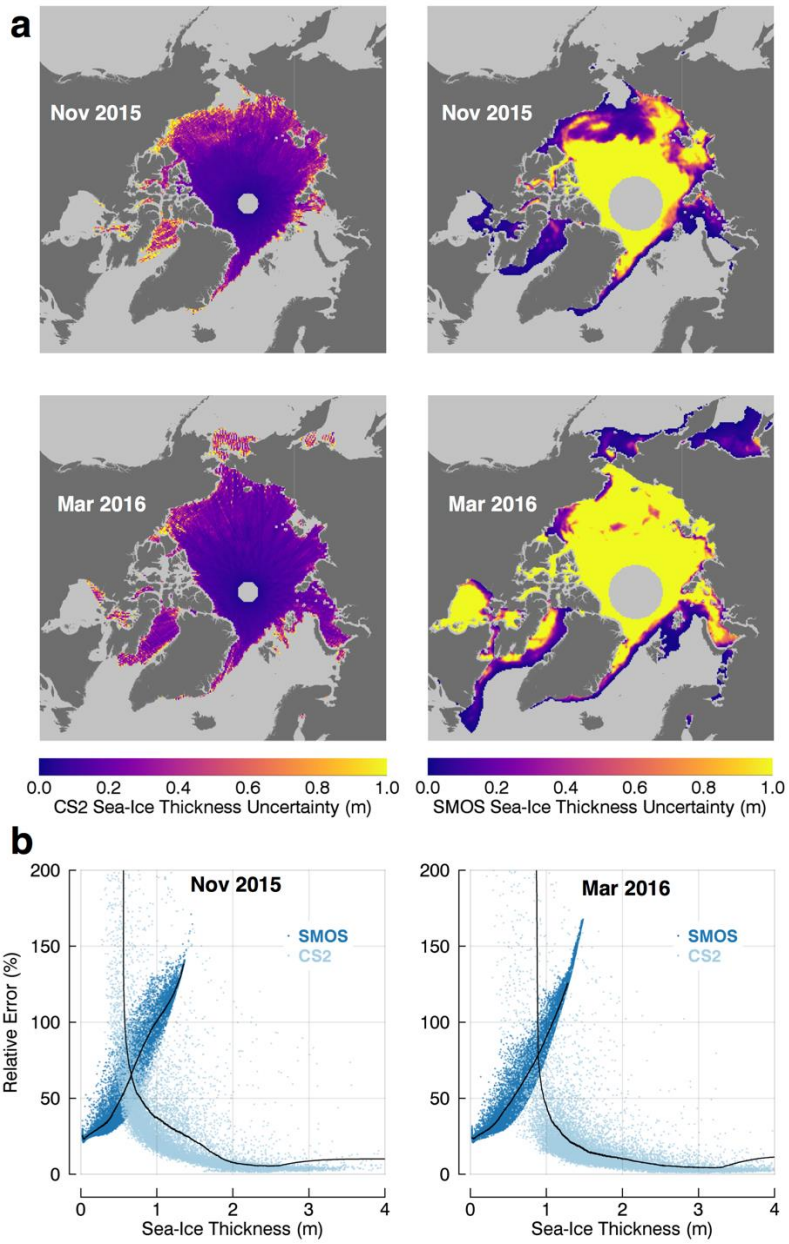

Figure 1: a) Monthly sea-ice thickness uncertainty maps of the CryoSat-2 and SMOS retrieval from November 2015 and March 2016. b) Relative uncertainties from November 2015 and March 2016. A running mean is represented by black solid lines.

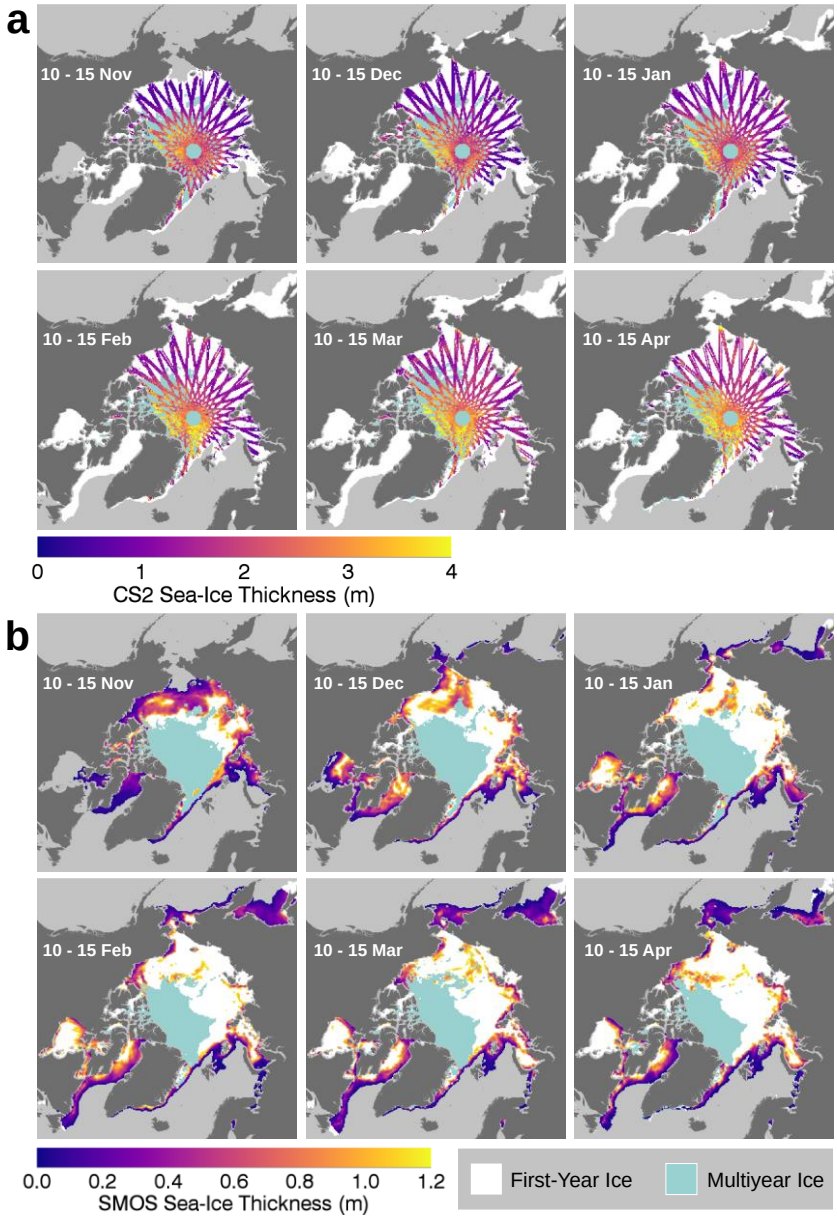

Figure 2: Weekly averaged data grids for the freezing season November-April 2015/16. a) Weekly CryoSat-2 retrieval as used for the optimal interpolation. b) Weekly means of daily SMOS ice thickness retrievals, cropped by a 1 m maximum SMOS thickness uncertainty filter. The background indicates first-year and multiyear ice coverage.

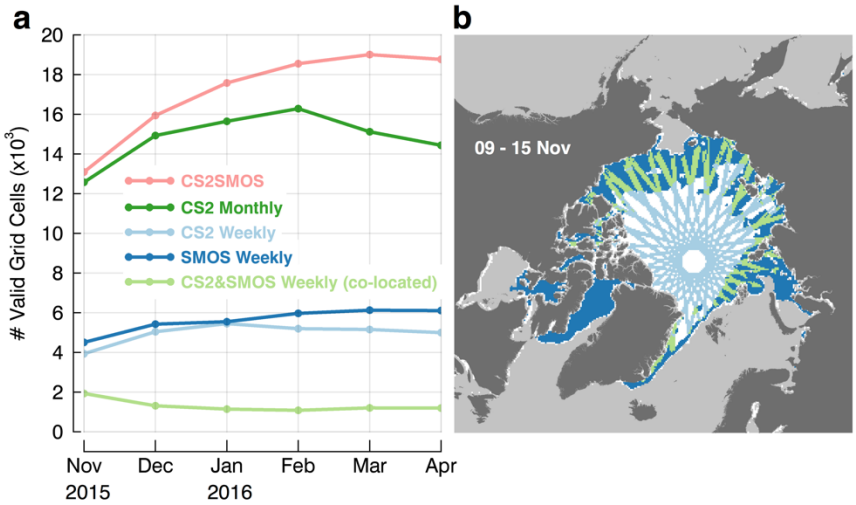

Figure 3: a) Spatial coverage in number of valid 25 km grid cells from November 2015 to April 2016. Here, 'valid' indicates grid cells that contain a valid thickness estimate. b) Spatial distribution of valid weekly thickness retrievals by CS2 (light blue) and SMOS (dark blue) during a week in November 2015. Co-located grid cells are highlighted in light green. The white background field indicates the reference ice extent.

3 CryoSat-2/SMOS merged product algorithm

3.1 Method

We use an optimal interpolation scheme (OI) like Böhme and Send (2005), Boehme et al. (2008), and McIntosh (1990) that allows the merging of datasets from diverse sources on a predefined analysis grid. The data are weighted differently based on known uncertainties of the individual products and modeled spatial covariances. OI minimizes the total error of observations and provides ideal weighting for the observations at each grid cell. The data merging methods were first described in Ricker et al. (2017). Here, we present the processing methods, on which the here presented optimal interpolation is based on. Figure 4 shows the processing scheme which will be described in more detail in the following.
The OI scheme is used to get an objective estimate of values at observed or unobserved locations. The basic equation is:

$$\mathrm{Z_a} = \mathrm{Z_b} + \mathbf{K}[\mathrm{Z_o} - \mathrm{H}(\mathrm{Z_b})], \quad (1)$$

where the vector $\mathrm{Z_a}$ is the analysis field that represents the merged CS2SMOS ice thickness retrieval which we aim for. $\mathrm{Z_b}$ is the background field vector and $\mathrm{Z_o}$ the vector that contains all SMOS and CS2 observations. **K** is a weight matrix. As observations we here define already gridded thickness estimates, based on weekly averages as shown in Figure 2. This approach reduces statistical uncertainties and provides equally distributed observations, which improves the performance of the OI. In addition, it is reasonable to reduce the number of observations, otherwise computing can become time-consuming. We assume that the observations are static, which is a simplification, because the satellite thickness estimates are temporally incoherent due to ice deformation and motion. Therefore, we neglect any temporal correlations. H is an operator that transforms the background field into the observation space. To be more specific, this is realized by an inverse distance interpolation method. We aim to retrieve weekly analysis fields that are updated daily. Melting does not allow to retrieve summer sea-ice thickness estimates neither from CS2 nor SMOS. Hence, the CS2SMOS product is limited to the period from mid-October to mid-April. The optimal interpolation, including input and output products, is carried out on the level of gridded data.

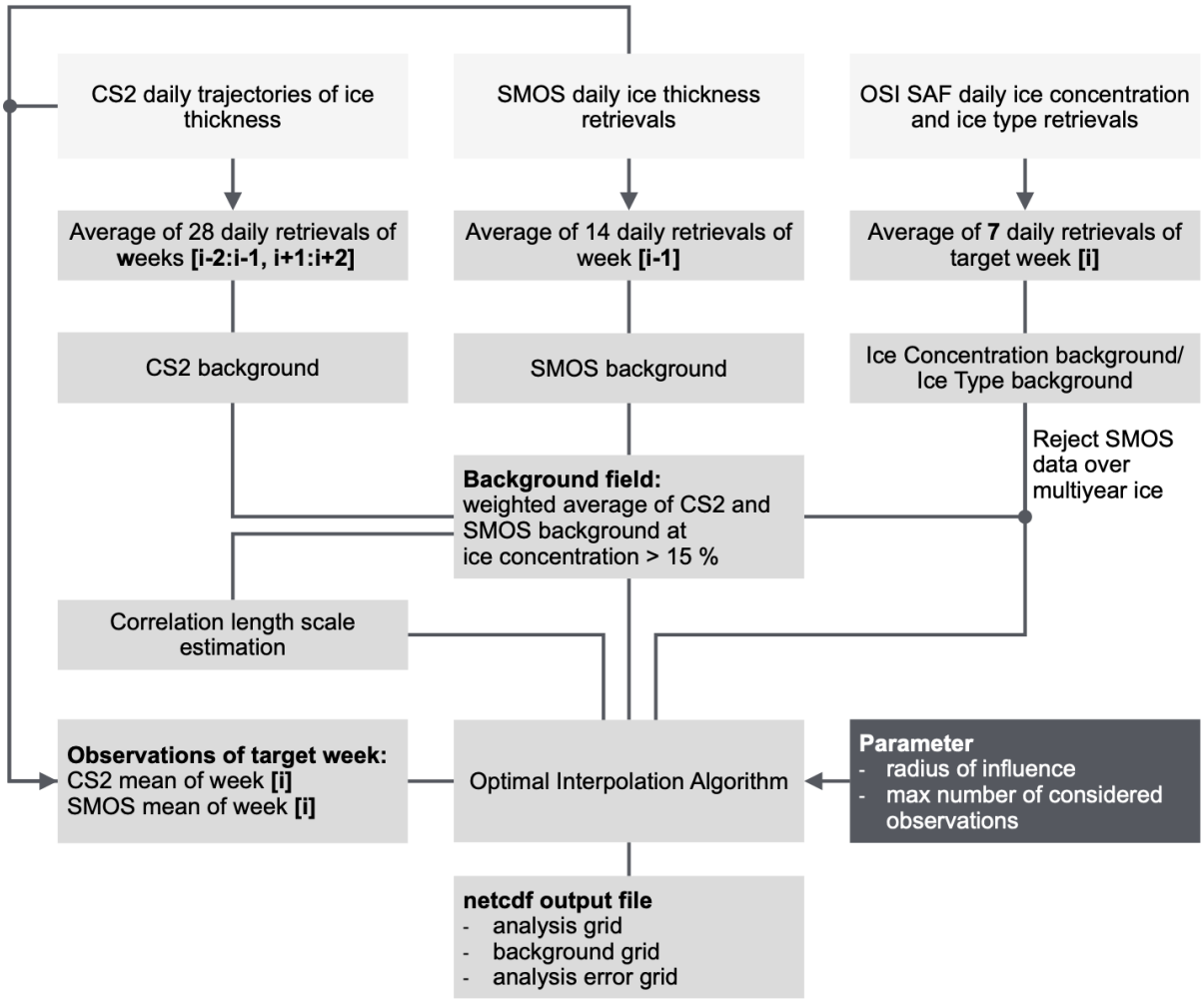

Figure 4: Optimal interpolation processing scheme. Week [i] represents the target week.

3.2 Grid

All source datasets (see section 3.3), are projected onto the 25 km EASE2 Grid (Figure 5), which is based on a polar aspect spherical Lambert azimuthal equal-area projection (Brodzik et al., 2012). The grid dimension is 5400 km x 5400 km, equal to a 432 x 432 grid. The grid is centered on the geographic Pole, meaning that the Pole is located at the intersection of center cells (Figure 5).

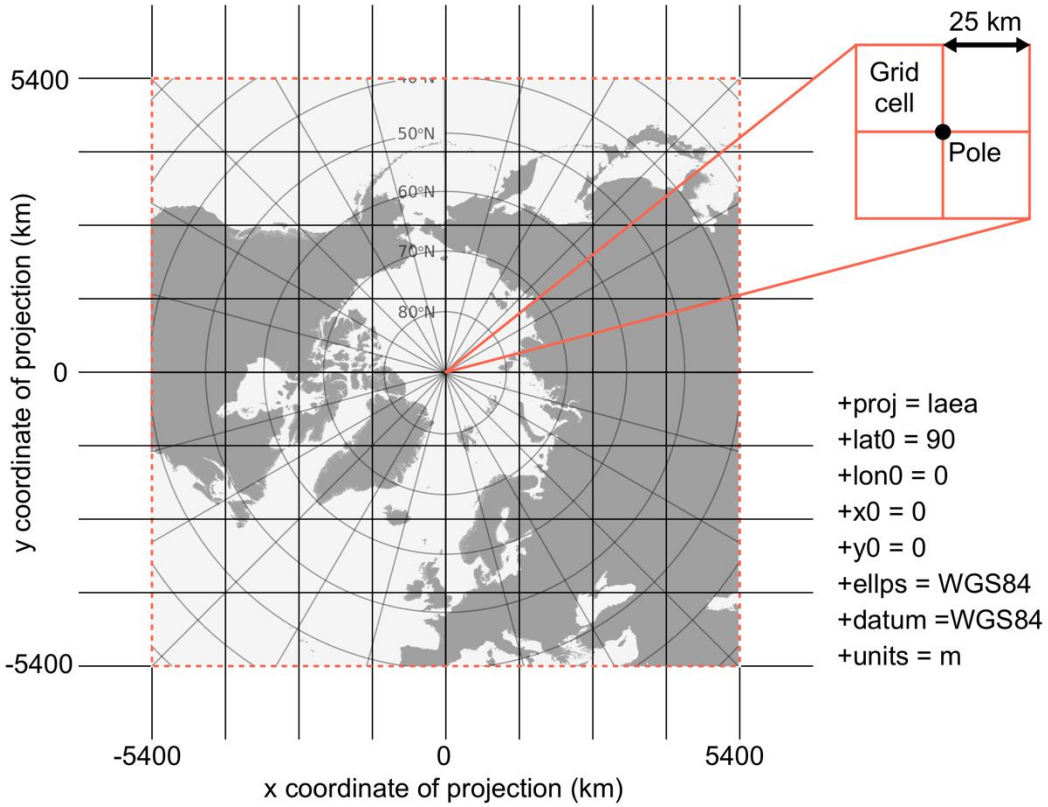

Figure 5: Specifications of the EASE2 25 km grid, which is used for the merged product.

3.3 Data Sources

For the data merging, we use the AWI CS2 product (processor version 2.6), and the AWI SMOS sea-ice thickness retrieval (processor version 3.3, Tian-Kunze et al., 2014; Kaleschke et al., 2016). Besides the sea ice thickness data, the data merging requires sea ice concentration and sea ice type (Identification of first year and multi-year sea ice) provided by the Ocean and Sea Ice Satellite Application Facility (OSI SAF). To avoid erroneous estimates outside areas where sea ice is ever likely to occur and to assure a consistent sea ice coverage throughout the data record, we apply an ocean/land mask. Table 1 summarizes the different input grids, their spatial resolution, and temporal sampling.

The change in version v206 is limited to an update of most recent version v2.6 of the CryoSat-2 sea ice thickness product, which included an improved sea ice type auxiliary data and a full reprocessing with the latest CryoSat-2 Level-1 data of algorithm baseline-E. In addition the near real-time latency of CryoSat-2 data production was increased from 36h to 48h to ensure full data availability on the production system.

Table 1: Properties of input and output data grids, which are used to obtain the merged product.

Product	**Source**	**Frequency**	**Spatial coverage**	**Grid/ resolution**
SMOS sea ice thickness v3.3	ftp.awi.de/sea_ice	Daily	Entire Arctic	Polarstereo 12.5 km
CS2 sea ice thickness (l2p) v2.6	ftp.awi.de/sea_ice	Daily	< 88N with gaps	Trajectory, 0.3km
Ice concentration (for operational mode) (OSI-401-b)	ftp://osisaf.met.no/ archive/ice/conc/	Daily	Entire Arctic	Polarstereo 10 km
Ice concentration (for reprocessing mode) (OSI SAF CDR/iCDR v3.0)	https://thredds.met.no/thredds/c3s/c3s_cdr_ice_conc_v2p0.html https://thredds.met.no/thredds/c3s/c3s_cdr_ice_type_v2p0.html	Daily	Entire Arctic	EASE2 25 km
Ice type (OSI-403-d)	ftp://osisaf.met.no/ archive/ice/type/	Daily	Entire Arctic	Polarstereo 10 km
Ocean/land mask	ftp://osisaf.met.no/ reprocessed/ice/ oceanmasks/	-	Entire Arctic	EASE2 12.5 km
Merged product v206	ftp.awi.de/sea_ice	Daily	Entire Arctic	EASE2 25 km

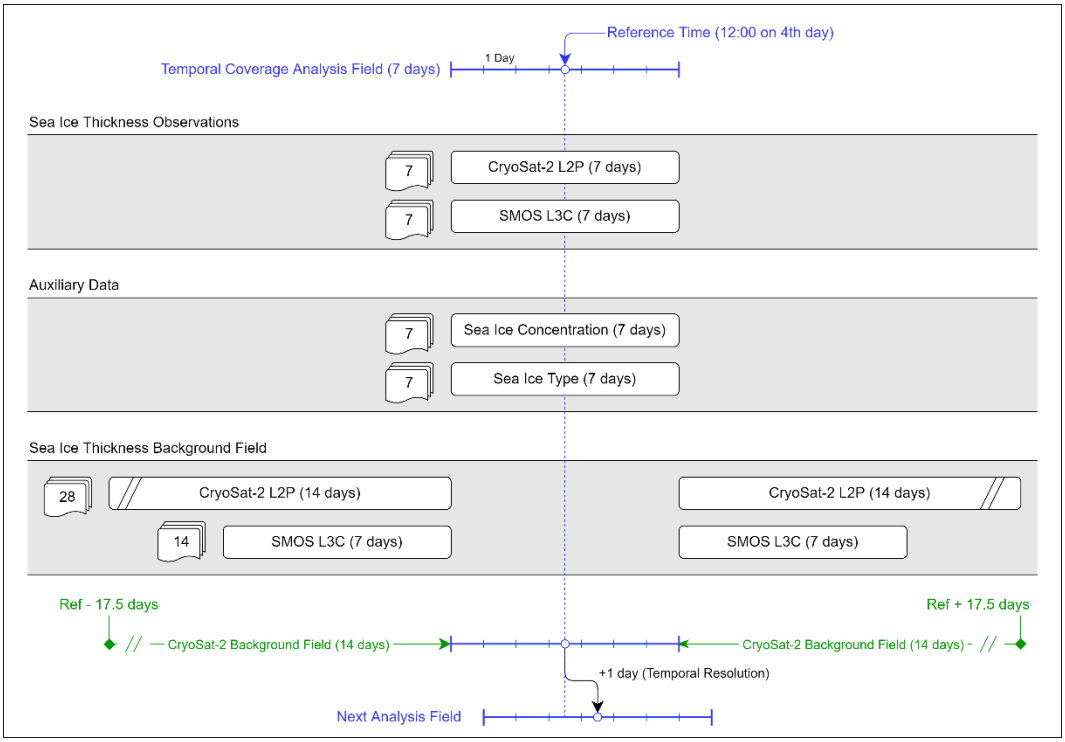

Figure 6: The scheme illustrates the usage of weekly input grids for the background field (reprocessing mode) and the observation field.

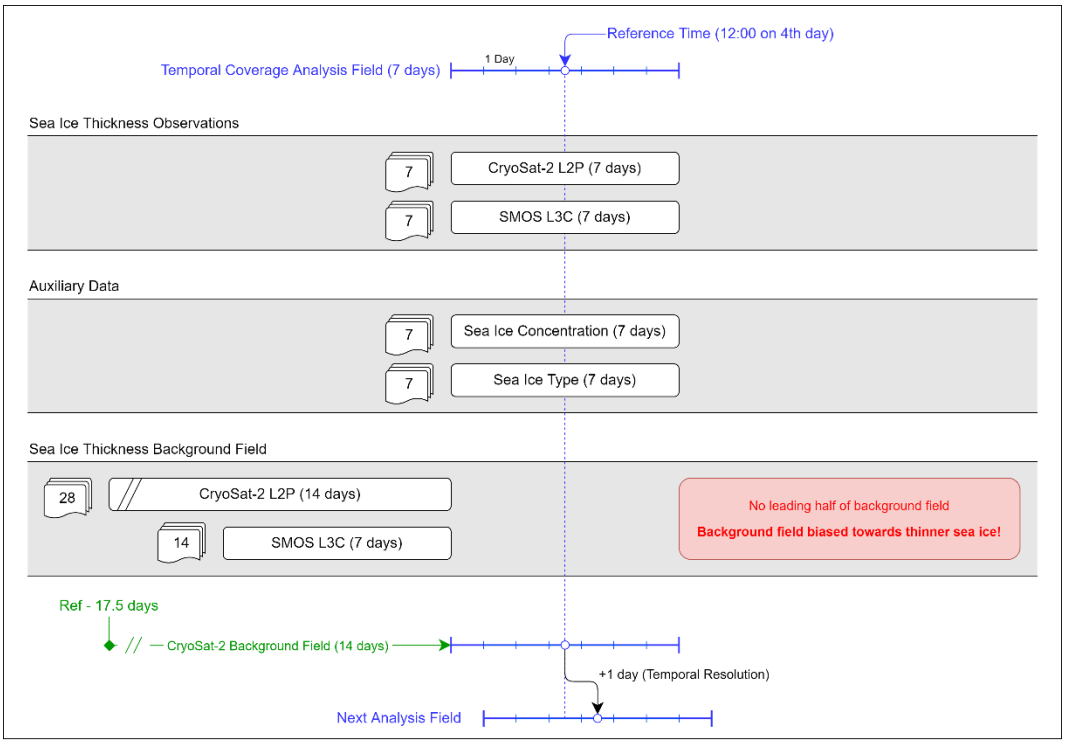

Figure 7: The scheme illustrates the usage of weekly input grids for the background field (operational mode) and the observation field.

3.4 Background field

We use daily trajectories (l2p) of sea ice thickness from CS2 that are collected for the background field of the reprocessed CS2SMOS product (Figure 6), ranging from 2 weeks

behind to two weeks ahead, to get a nearly complete background field coverage for the Central Arctic at a certain target week (Figure 4). Since version v202, the target weeks do not coincide only with calendar weeks but is updated in daily increments. To ensure an independent background field, the target week itself is not included. For the same reason, we use a SMOS contribution to the background field from the week before and after the target week. For the operational mode the target week includes the most recent available data and therefore only CS2 or SMOS data before the target week can contribute to the background field (Figure 7).

The initial background field is represented by a weighted average:

$$\overline{Z} = \frac{Z_{cs2}/\sigma^2_{cs2} + Z_{smos}/\sigma^2_{smos}}{1/\sigma^2_{cs2} + 1/\sigma^2_{smos}} \quad (2)$$

Z is the sea-ice thickness and σ the statistical uncertainty included in the CS2 and SMOS source datasets. . Since we use CS2 and SMOS retrievals for the background field beyond the target week and because the SMOS composite contains artifacts of thin ice (< 10 cm) in coastal regions, we additionally use an ice concentration mask, likewise a weekly mean of the OSI SAF ice concentration product to determine the ice coverage during the target week. Here, we apply a threshold of 15 % and only grid cells that exceed this value will be considered as ice covered, which corresponds to the ice extent products provided by OSI SAF and the National Snow and Ice Data Center (NSIDC). Gaps in the weighted average, derived from Eq. 2, are interpolated by using a nearest neighbor scheme. At this stage we use the background field for the estimation of the correlation length scale (next section). To finally obtain Z_b we reduce the noise by applying a smoothing filter, using radial averaging with a 25 km radius, and before it is applied in the optimal interpolation algorithm. After filtering we obtain Z_b as it is used in Eq. 1.

3.5 Correlation Length Scale Estimation

The correlation length scale ξ controls the impact of a data point on the analysis grid point depending on the distance. Considering the grid resolution of 25 km, we aim for large scale correlations. Ideally, our correlation length scale estimate is large in the center of a certain ice type regime with similar ice thickness (i.e., level FYI). On the other hand, we expect a low ξ

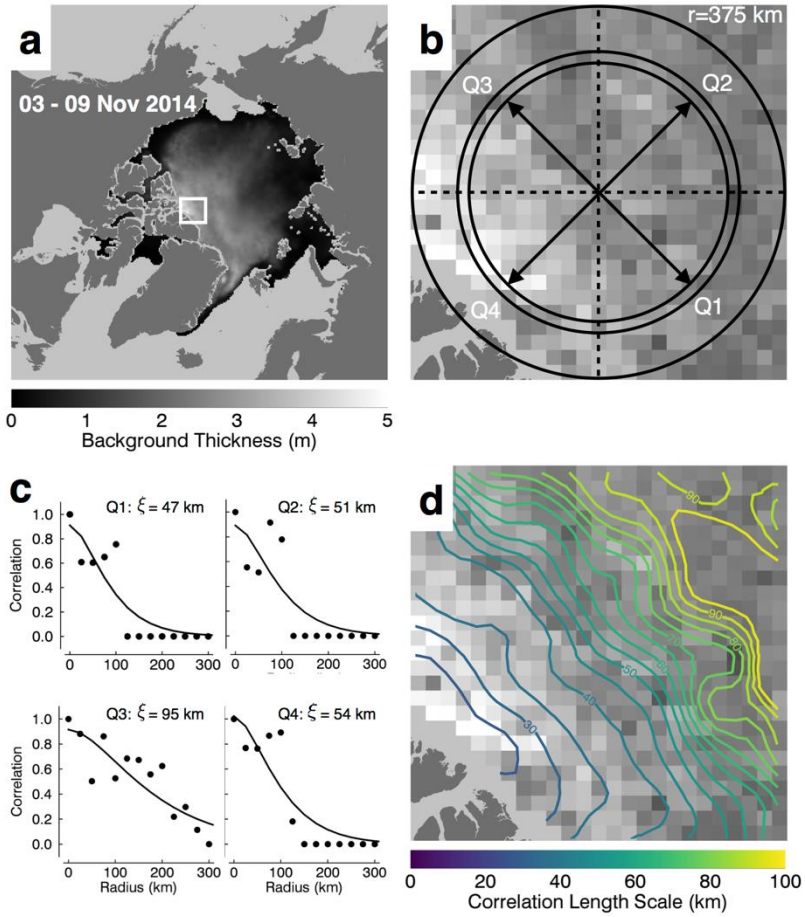

Figure 8: Scheme for the estimation of the correlation length scale ξ for a single grid cell for the target week 3-9 November 2014. a) Background field with indicated area of interest (white box). b) Adjacent ice thickness grid cells within a radius of 375 km are binned into annuli of distance and 4 quadrants. (c) Binned thickness estimates are used to calculate the structure function of each quadrant. ξ is estimated by fitting an exponential function. d) Contour map of estimated correlation length scales for the considered area.

value at locations with varying thickness gradients. Figure 7 illustrates the estimation of ξ for a certain grid cell Z_0 in the Lincoln Sea during a week in November. To estimate ξ, we consider the unfiltered background field Z_b (Figure 7a), which means that the smoothing described in 3.4 is not applied. In the following, we define a structure function ϵ^2, which is related to the normalized auto correlation function R(d,Q) as follows (Böhme & Send, 2005):

$$\epsilon^2(\mathrm{d,Q}) = \overline{\left(Z_0^{'} - Z_{\mathrm{Q,d}}^{'}\right)^2} = 2\overline{\sigma_{Z'}^2} - 2\overline{\sigma_{Z'}^2}\mathrm{R(d,Q)} \quad (3)$$

$$\mathrm{R(d,Q)} = 1 - \frac{\epsilon^2(\mathrm{d,Q})}{2\overline{\sigma_{Z'}^2}} \quad (4)$$

Quadrants Q are defined to accommodate the anisotropy of the spatial ice thickness distribution (Figure 7b). $\epsilon^2(\mathrm{d,Q})$ represents the square differences between ice thickness of the center grid cell and the ice thickness of the grid cells of binned 25 km distances d away from the center grid cell, in a quadrant Q. $Z_{\mathrm{Q,d}}^{'}$ is the unfiltered background thickness, binned according to d and Q, meaning the average of all background thickness grid cells within

Quadrant Q within the bin edges (see Figure 7b). Figure 7b reveals the annuli of distance and the 4 Quadrants. $\sigma_{Z'}^2$ are the corresponding mean variances of a certain quadrant.

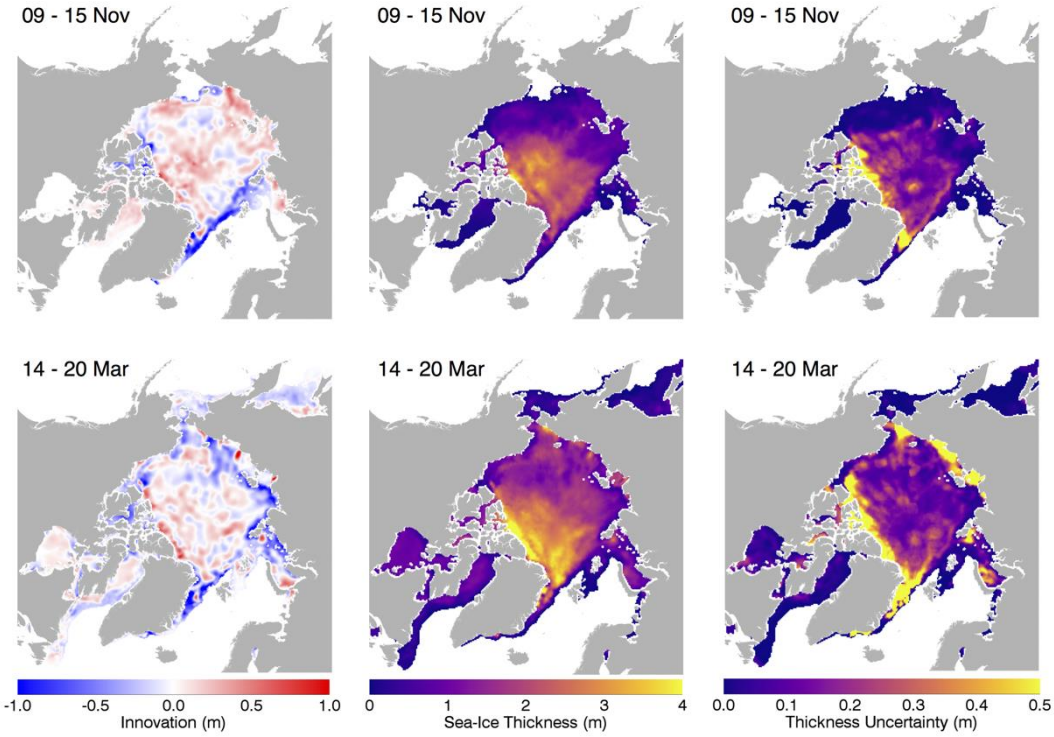

Figure 9: Output grids from the optimal interpolation processing for weeks in November 2015 and March 2016: The innovation (left column) is the difference between background and the merged product ice thickness (center column). The sea-ice thickness uncertainty of the optimal interpolation product is derived from the relative analysis error, scaled with the observation variances (right column).

With Eq. 4 we then obtain the auto correlation function $\mathrm{R(d,\,Q)}$, which is computed up to radius of 750 km (30 bins). In the next step, we fit a function of the form:

$$C(d,\xi) = \left(1 + \frac{\mathrm{d}}{\xi}\right)\exp\left(\frac{\text{-d}}{\xi}\right) \tag{5}$$

with a non-linear least squares approach to R(d,Q) and obtain an estimate for ξ. Figure 7c shows the calculated auto correlation function R(d,Q) and the functional fit (Eq. 5). A stronger decay of R(d,Q) occurs with rising deviation between Z_0 and the thickness at a certain distance in a certain quadrant. R(d,Q) can also become negative if $\epsilon^2(\mathrm{d,Q})$ / $2\overline{\sigma_{Z'}^2}$ becomes >1. In order to improve the fitting performance, we set R(d,Q) = 0 if R(d,Q) becomes < 0. Furthermore, ξ is rejected if the computation fails. Finally, we average the ξ values from the 4 quadrants. In order to remove outliers and noise, the derived ξ grid is low-pass filtered with a smoothing radius of 25 km. Grid cells with failed computation are interpolated by a nearest neighbor scheme afterwards. Figure 7d shows the spatial correlation length scales ξ for 3-9 November 2014. It highlights the sensitivity to changing thickness gradients as ξ decreases towards the coast of the Canadian Archipelago, where higher sea ice thickness gradients likely occur due to increased deformation.

3.6 Optimal interpolation

The weight matrix **K**, which is needed for the computation of Z_a, is retrieved by the background error covariance matrix **B** in the observation space, multiplied by the inverted total error covariance matrix:

$$\mathbf{K}=\mathbf{B}\mathbf{H}^{\mathrm{T}}\left(\mathbf{R}+\mathbf{H}\mathbf{B}\mathbf{H}^{\mathrm{T}}\right)^{-1}, \tag{6}$$

where **R** is the error covariance matrix of the observations. To reduce computation expense, we assume the following:

1. We neglect correlations of observation errors which means that **R** is a matrix with non-zero elements only on the diagonal. These variances are represented by the SMOS and CS2 product uncertainties.
2. We assume that the influence of observations that are located far away from the analysis grid point can be neglected. Therefore, instead of computing the entire covariance matrix, we only consider observations within a radius of influence. This radius is set to 250 km to gather just enough observations in regions which large gaps, for example over MYI between two CS2 orbits where valid SMOS observations are not available.
3. To further reduce computation expense, we limit the number of matched observations to 120, meaning that in the case of more matches, only the 120 closest observations are considered.
4. We generally assume that all observations are unbiased.

$\mathbf{B}\mathbf{H}^{\mathrm{T}}$ and $\mathbf{H}\mathbf{B}\mathbf{H}^{\mathrm{T}}$ are estimated using the correlation function in Eq. 5:

$$(bh^T)_i = \left(1 + \frac{d\left(x_{o_i}, x_{a_{m,n}}\right)}{\xi_{m,n}}\right) exp\left(\frac{-d\left(x_{o_i}, x_{a_{m,n}}\right)}{\xi_{m,n}}\right)$$

$$(hbh^T)_{i,j} = \left(1 + \frac{d\left(x_{o_i}, x_{o_j}\right)}{\xi_{m,n}}\right) exp\left(\frac{-d\left(x_{o_i}, x_{o_j}\right)}{\xi_{m,n}}\right) \tag{7}$$

$$d(x, y) = \|x - y\| \tag{8}$$

Here, x_{o_i} and $\mathrm{x}_{\mathrm{o_j}}$ represent the locations of the matched observations within the radius of influence. $x_{a_{m,n}}$ refers to the location of the analysis grid cell. Because of Eq. 7, the impact of a data point decreases with increasing distance. The estimation of ξ is described in section 3.2.4.

Computing $\mathbf{B}\mathbf{H}^{\mathrm{T}}$ and $\mathbf{H}\mathbf{B}\mathbf{H}^{\mathrm{T}}$ allows the computation of the weight matrix **K**. Thus, we retrieve the second part of Eq. 1, which is called *innovation*. This iterative procedure is accomplished for each analysis grid cell, leading to the complete analysis grid $\mathrm{Z_a}$.

3.7 The Analysis Error Field

The corresponding analysis error covariances are derived by:

$$\sigma^2_{Z_a} = (\mathbf{I}\text{-}\mathbf{KH})\mathbf{B} \quad (9)$$

Since we consider variances exclusively, we only calculate the diagonal elements of $\sigma^2_{Z_a}$. Figure 8 shows the merged product and furthermore the innovation field and the analysis error, which is the root of the error variance. The analysis thickness uncertainty is a relative quantity ranging between 0 and 1, scaled with observation variances. It increases where the weekly CS2 retrieval leaves gaps and where valid SMOS observations are not available, for example at the North Pole or over MYI. In this case the analysis heavily depends on the background field, and therefore the error increases. For validation of the merged product, we refer to Ricker et al. (2017), and the RM-TN.

3.8 Product Changelog

The CryoSat-2/SMOS product is updated annually. The updates compared to earlier versions are outlined below.

System Update	Updates of input data sets and other technical evolutions concerning file format and product metadata
Algorithm Update	Evolution of the CryoSat-2/SMOS merging algorithm

3.8.1 Version 206 – System Update (Release 13.11.2023)

- Update of CryoSat-2 L2P input (from version 2.5 to version 2.6). Changes include:
  - Reprocessing with CryoSat-2 ICE Level-1b algorithm baseline-E (in v2.5, baseline-E data was only used since Oct 2020).
  - Use the OSI-SAF / C3S sea ice type (interim) climate data record. Notable changes in sea ice type information in the first half of October.
  - There had been cases of incomplete CryoSat-2 near real-time L1B data on the production system in v2.5. The latency of near real-time production has been increased from 36h to 48h

3.8.2 Version 205 – System Update (Release 26.10.2022)

- Update of CryoSat-2 L2P input (from version 2.4 to version 2.5). Changes include:
  - Surface type classification evolution to include more data from thin ice / mixed ice conditions. The result is more available data.
  - Addition of marginal ice zone flag that indicates unrealistic high thickness values in the presence of ocean waves/swell penetrating the ice cover.

  - Resolved issue with orbit segment connectivity leading to data loss the CryoSat-2 v2.4
  - Resolved issue with computation of waveform pulse peakiness for noisy waveforms potentially leading to incorrect surface type classications
- Apply CryoSat-2 marginal ice zone filter flag in CS2SMOS data merging

3.8.3 Version 204 – System Update (Release 21.10.2021)

- Update of CryoSat-2 L2P input (from version 2.3 to version 2.4). Changes include:
  - Latest CryoSat-2 L1B data version (ICE baseline-E from Oct. 2021 and later, ICE baseline-D until April 2021)
  - latest version of OSI-SAF sea ice concentration and sea ice type auxiliary data,
  - change of sea ice concentration mask from 70% to 15%)
- Update of SMOS L3C input (from version 3.2 to version 3.3). Changes include:
  - Latest SMOS L1C data version (v724)
  - Grid: NSIDC Sea Ice Polar Stereographic North (EPSG:3411) has been replaced by WGS 84 / NSIDC Sea Ice Polar Stereographic North (EPSG:3413)
- CS2SMOS file format changes
  - Minor update of global attributes

3.8.4 Version 203 – System Update (Release 15.10.2020)

- Update of CryoSat-2 L2P input (from version 2.2 to version 2.3). Changes include:
  - Latest CryoSat-2 L1B data version (ICE baseline-D) for full data record
  - Updated auxiliary data sets
    - OSI-SAF sea ice concentration climate data record (version 1.2 to 2.0)
    - Reverted mean sea surface from DTU18 to DTU15
    - Optimized sea-ice type information near coasts and in the Canadian Archipelago
  - Algorithm Evolution:
    - Updated handling of snow depth and density

3.8.5 Version 202 – System and Algorithm Update (Release 27.09.2019)

- time coverage resolution has been changed from 7 days to 1 day, e.g., daily updates with a data period of 7 days
- Update of CryoSat-2 L2P input (from version 2.1 to version 2.2).
- Update of SMOS L3C input (from version 3.1 to version 3.2), which is now processed and provided by AWI.
- Added ocean mask to allow for a consistent land/ocean mask throughout the entire data record to overcome inconsistencies due to switches of the land masks in the OSI SAF ice concentration products.
- Use of dedicated sea ice concentration products for the operational mode and for the reprocessing mode. In the operational mode, we use the operational OSI-401 ice

concentration product, while in the reprocessing mode, the reprocessed OSI -430-b ice concentration product is used. Both are provided by OSI SAF.

- Changes in the NetCDF variable names, fulfilling CF 1.6 conventions

3.8.6 Version 201 – Official ESA Release (Release 15.10.2018)

See [ATBD1]

4 Product description

This chapter provides an overview of the output data format. For a more detailed description, we refer to the PDD.

4.1 Overview

Parameter	Sea ice thickness
Spatial coverage	N: 90°, S:16.6°, E:180°, W: -180°
Spatial resolution	25 km x 25 km
Temporal data record coverage:	November 2010 to present
Temporal average window	7 days
Time coverage resolution	1 day
Data format(s)	NetCDF
Platforms	CryoSat-2, SMOS
Version	v206

4.2 File naming convention

NetCDF files are named using the following convention:
`<convention-prefix>_<regional code>-<institution>,<platform(s)>,<grid>_<time>_<mode>_<product version>_<file version>.nc`

`convention-prefix`	World Meteorological Organization: `W`
`regional code`	European: `XX`
`institution`	European Space Agency: `ESA`
`processing level/parameter`	level 4 sea ice thickness: `l4sit`
`platform(s)`	Satellites: `SMOS, CS2`
`grid`	25 km EASE2 grid, Northern Hemisphere: `NH_25KM_EASE2`
`time`	time span: `yyyymmdd - yyyymmdd`
`mode`	reprocessing: `r`, operational: `o`
`product version`	version 2.0.6: `v206`
`file version`	version 1: `01`

Example NetCDF naming for operationally processed data:
`W_XX-ESA,SMOS_CS2,NH_25KM_EASE2_20190304_20190310_o_v206_01_l4sit.nc`

Example NetCDF naming for reprocessed data:
`W_XX-ESA,SMOS_CS2,NH_25KM_EASE2_20190304_20190310_r_v206_01_l4sit.nc`

4.3 File Format

The weekly grids are given in standardized binary data format (Network common data form: NetCDF v4). Global attributes are given in Table 2. The variables are given as grid arrays, see, therefore Table 3. NetCDF files are formatted according to CF conventions: CF-1.6 ACDD-1.3. We use a scaling factor of 10^-3 and a fillvalue = -2147483647.

Table 2: Global attributes from an example NetCDF file, from March 4 to March 10, 2019.

Attribute	Value
title	Sea Ice Thickness derived from merging CryoSat-2 and SMOS ice thickness
description	Weekly Arctic sea-ice thickness derived from CryoSat-2 and SMOS using an optimal interpolation scheme
summary	Weekly Arctic sea-ice thickness derived from CryoSat-2 and SMOS using an optimal interpolation scheme
keywords	Cryosphere > Sea Ice > Sea Ice Thickness
product_version	206
processing_mode	r
time_of_creation	Fri Jun 21 10:30:37 2019
history	Fri Jun 21 10:30:37 2019 creation
Conventions	CF-1.6 ACDD-1.3
spatial_resolution	25.0 km grid spacing
geospatial_lat_min	16.623929977416992
geospatial_lat_max	90.0
geospatial_lon_min	-180.0
geospatial_lon_max	180.0
geospatial_vertical_min	0.0
geospatial_vertical_max	0.0
time_coverage_start	2019-03-04T00:00:00Z
time_coverage_end	2019-03-11T00:00:00Z
time_coverage_duration	P7D
time_coverage_resolution	P1D
platform	CryoSat-2, SMOS
project	CS2SMOS PDS: SMOS & CryoSat-2 Sea Ice Data Product Processing and Dissemination Service
institution	Alfred-Wegener-Institut Helmholtz Zentrum für Polar und Meeresforschung (AWI), http://www.awi.de
creator_name	Alfred-Wegener-Institut Helmholtz Zentrum für Polar und Meeresforschung (AWI), http://www.awi.de
creator_type	institution
creator_url	www.awi.de
contributor_name	Robert Ricker, Stefan Hendricks, Xiangshan Tian-Kunze, Lars Kaleschke
contributor_role	PrincipalInvestigator, Author, Author, Author
publisher_email	cs2smos-support@awi.de
Publisher_url	http://spaces.awi.de/confluence/x/DwVmEQ

references	Ricker, R., Hendricks, S., Kaleschke, L., Tian-Kunze, X., King, J., and Haas, C.: A weekly Arctic sea-ice thickness data record from merged CryoSat-2 and SMOS satellite data, The Cryosphere, 11, 1607-1623, https://doi.org/10.5194/tc-11-1607-2017, 2017.
_CoordSysBuilder	ucar.nc2.dataset.conv.CF1Convention

Table 3: NetCDF file variables and their attributes. Type "int" refers to 32-bit long signed integer.

Variable	Attributes	Type	Dimension
Lambert_Azimuthal_Grid	:grid_mapping_name: lambert_azimuthal_equal_area :longitude_of_projection_origin: 0.0 :latitude_of_projection_origin: 90.0 :false_easting: 0.0 :false_northing: 0.0 :semi_major_axis: 6378137.0 :inverse_flattening: 298.25723 :proj4_string: +proj=laea +lon_0=0 +datum=WGS84 +ellps=WGS84 +lat_0=90.0	int	-
time	:units: seconds since 1978-01-01 00:00:00 :long_name: reference time of product :standard_name: time :axis: T :calendar: standard :bounds: time_bnds	double	1
time_bnds	:units: seconds since 1978-01-01 00:00:00	double	1,2
xc	:units: km :long_name: x coordinate of projection (eastings) :standard_name: projection_x_coordinate	double	
yc	:units: km :long_name: y coordinate of projection (northings) :standard_name: projection_y_coordinate	double	1,432,432
lon	:units: degrees_east :long_name: longitude coordinate :standard_name: longitude	float	1,432,432
lat	:units: degrees_north :long_name: latitude coordinate :standard_name: latitude	float	1,432,432
analysis_sea_ice_thickness	:units: m :long_name: CS2SMOS merged sea ice thickness :standard_name: sea_ice_thickness :grid_mapping: Lambert_Azimuthal_Grid :coordinates: time lat lon :scale_factor: 0.001 :valid_min: :valid_max: :_FillValue: -2147483647	int	1,432,432

background_sea_ice_thickness	:units: m :long_name: optimal interpolation background field :standard_name: sea_ice_thickness :grid_mapping: Lambert_Azimuthal_Grid :coordinates: time lat lon :scale_factor: 0.001 :valid_min: :valid_max: :_FillValue: -2147483647	int	1,432,432
weighted_mean_sea_ice_thickness	:units: m :long_name: weighted mean of weekly cs2 and smos ice thickness retrievals :standard_name: sea_ice_thickness :grid_mapping: Lambert_Azimuthal_Grid :coordinates: time lat lon :scale_factor: 0.001 :valid_min: :valid_max: :_FillValue: -2147483647	int	1,432,432
innovation	:units: m :long_name: difference between background and analysis ice thickness :grid_mapping: Lambert_Azimuthal_Grid :coordinates: time lat lon :scale_factor: 0.001 :valid_min: :valid_max: :_FillValue: -2147483647	int	1,432,432
sea_ice_ concentration	:units: % :long_name: sea ice concentration :standard_name: sea_ice_area_fraction :grid_mapping: Lambert_Azimuthal_Grid :source: OSI-430-b :source_product_version: 2.0 :coordinates: time lat lon :scale_factor: 0.01 :valid_min: :valid_max: :_FillValue: -2147483647	int	1,432,432
sea_ice_type	:long_name: sea ice type :standard_name: sea_ice_classification :grid_mapping: Lambert_Azimuthal_Grid :source: OSI-403 :source_product_version: 4.0 :coordinates: time lat lon :_FillValue: -2147483647 :flag_values: 2 :flag_values: 3 :flag_meanings: first_year_ice :flag_meanings: multi_year_ice :flag_descriptions: 2 -> relatively young ice\n 3 -> ice that survived a summer melt	int	1,432,432

correlation_length_scale	:units: m :long_name: correlation length scale of sea ice thickness :grid_mapping: Lambert_Azimuthal_Grid :coordinates: time lat lon :valid_min: :valid_max: :_FillValue: -2147483647	int	1,432,432
analysis_sea_ice_thickness_unc	:units: m :long_name: uncertainty of the merged sea ice thickness :grid_mapping: Lambert_Azimuthal_Grid :coordinates: time lat lon :scale_factor: 0.001 :valid_min: :valid_max: :_FillValue: -2147483647	int	1,432,432
smos_sea_ice_thickness	:units: m :long_name: weekly averaged SMOS ice thickness :standard_name: sea_ice_thickness :grid_mapping: Lambert_Azimuthal_Grid :source: SMOS-Icethickness :source_product_version: 3.3 :coordinates: time lat lon :scale_factor: 0.001 :valid_min: :valid_max: :_FillValue: -2147483647	int	1,432,432
cryosat_sea_ice_thickness	:units: m :long_name: weekly averaged CryoSat-2 ice thickness :standard_name: sea_ice_thickness :grid_mapping: Lambert_Azimuthal_Grid :source: AWI Sea Ice Radar Altimetry (SIRAL) :source_product_version: 2.6 :coordinates: time lat lon :scale_factor: 0.001 :valid_min: :valid_max: :_FillValue: -2147483647	int	1,432,432

5 References

Boehme, L., Meredith, M. P., Thorpe, S. E., Biuw, M., and Fedak, M.: Antarctic Cir- cumpolar Current frontal system in the South Atlantic: Monitoring using merged Argo and animal-borne sensor data, Journal of Geophysical Research: Oceans, 113, doi: 10.1029/2007JC004647, URL http://dx.doi.org/10.1029/2007JC004647, c09012, 2008.

Böhme, L. and Send, U.: Objective analyses of hydrographic data for referencing profiling float salinities in highly variable environments, Deep Sea Research Part II: Topical Studies in Oceanography, 52, 651–664, 2005.

Brodzik, M. J., Billingsley, B., Haran, T., Raup, B., and Savoie, M. H.: EASE-Grid 2.0: Incremental but Significant Improvements for Earth-Gridded Data Sets, ISPRS International Journal of Geo-Information, 1, 32–45, doi:10.3390/ijgi1010032, URL http://www.mdpi.com/2220-9964/1/1/32, 2012.

Hendricks, S., Ricker, R., and Helm, V.: User Guide - AWI CryoSat-2 Sea Ice Thickness Data Product (v1.2), 2016.

Kaleschke, L., Tian-Kunze, X., Maaß, N., Beitsch, A., Wernecke, A., Miernecki, M., Müller, G., Fock, B. H., Gierisch, A. M., Schlünzen, K. H., Pohlmann, T., Dobrynin, M., Hen- dricks, S., Asseng, J., Gerdes, R., Jochmann, P., Reimer, N., Holfort, J., Melsheimer, C., Heygster, G., Spreen, G., Gerland, S., King, J., Skou, N., Søbjærg, S. S., Haas, C., Richter, F., and Casal, T.:SMOS sea ice product: Operational application and validation in the Barents Sea marginal ice zone, Remote Sensing of Environment, 180, 264-273, doi:http://dx.doi.org/10.1016/j.rse.2016.03.009, special Issue: ESA’s Soil Moisture and Ocean Salinity Mission - Achievements and Applications, 2016.

McIntosh, P. C.: Oceanographic data interpolation: Objective analysis and splines, Journal of Geophysical Research: Oceans (1978–2012), 95, 13 529–13 541, 1990.

Ricker, R., Hendricks, S., Helm, V., Skourup, H., and Davidson, M.: Sensitivity of CryoSat-2 Arctic sea-ice freeboard and thickness on radar-waveform interpretation, The Cryosphere, 8, 1607–1622, doi:10.5194/tc-8-1607-2014, 2014.

Ricker, R., Hendricks, S., Kaleschke, L., Tian-Kunze, X., King, J., Haas, C. (2017). A weekly Arctic sea-ice thickness data record from merged CryoSat-2 and SMOS satellite data. The Cryosphere, 11, 1607-1623.

Tian-Kunze, X., Kaleschke, L., Maaß, N., Mäkynen, M., Serra, N., Drusch, M., and Krumpen, T.: SMOS-derived thin sea ice thickness: algorithm baseline, product specifications and initial verification, The Cryosphere, 8, 997–1018, doi:10.5194/ tc-8-997-2014, URL http://www.the-cryosphere.net/8/997/2014/, 2014.